Supplementary Information

Inherent spin–polarization coupling in a magnetoelectric vortex

Sujit Das,*[$1] Valentyn Laguta,*[2] Katherine Inzani,*[3,4,5] Weichuan Huang,[6] Junjie Liu,[7] Ruchira Chatterjee,[3] Margaret R. McCarter,[8] Sandhya Susarla,[3] Arzhang Ardavan,[7] Javier Junquera,[9] Sinéad M. Griffin,[3,4] and Ramamoorthy Ramesh[3,6,8]

[1] Material Research Centre, Indian Institute of Science, Bangalore, 560012, India

[2] Institute of Physics of the Czech Academy of Sciences, Cukrovarnická 10, 162 00 Prague, Czech Republic

[3] Materials Sciences Division, Lawrence Berkeley National Laboratory, Berkeley, California 94720, USA

[4] Molecular Foundry, Lawrence Berkeley National Laboratory, Berkeley, California 94720, USA

[5] School of Chemistry, University of Nottingham, University Park, Nottingham, NG7 2RD, United Kingdom

[6] Department of Materials Science and Engineering, University of California, Berkeley, California 94720, USA

[7] CAESR, Department of Physics, University of Oxford, The Clarendon Laboratory, Parks Road, Oxford OX1 3PU, United Kingdom

[8] Department of Physics, University of California, Berkeley, California 94720, USA

[9] Departamento de Ciencias de la Tierra y Física de la Materia Condensada, Universidad de Cantabria, Cantabria Campus Internacional, Avenida de los Castros s/n, E-39005 Santander, Spain

(* authors contributed equally to this work)

[$]Corresponding author's email: sujitdas@iisc.ac.in

Methods

Sample preparation using RHEED-assisted pulsed-laser deposition. [*16 uc* $Pb_{1.2}Ti_{0.99}Fe_{0.01}O_3$/16 uc $SrTiO_3$]$_8$ superlattice (total 100nm) and 50nm $Pb_{1.2}Ti_{0.99}Fe_{0.01}O_3$ layer were synthesized on single-crystalline $DyScO_3$ (110) substrates *via* reflection high-energy electron diffraction (RHEED)-assisted pulsed-laser deposition (KrF laser). The $Pb_{1.2}Ti_{0.99}Fe_{0.01}O_3$ and $SrTiO_3$ layers were grown at 580 °C in 100 mTorr oxygen pressure. The laser fluence was 1.5 J/cm^2 with a repetition rate of 10 Hz. RHEED was used during the deposition to ensure the maintenance of a layer-by-layer growth mode for the $Pb_{1.2}Ti_{0.99}Fe_{0.01}O_3$ and $SrTiO_3$ as RHEED oscillation shown in supplementary Figure 1. The specular RHEED spot was used to monitor the RHEED oscillations. After deposition, the thin films were annealed for 10 minutes in 50 Torr oxygen pressure to promote full oxidation and then cooled down to room temperature at that oxygen pressure.

Structural analysis. In order to obtain a comprehensive picture of the crystal structure of the films, as well as information on the in-plane and out-of-plane ordering, structural characterization was done using synchrotron-based XRD at room temperature and 80K. The synchrotron XRD studies were performed at the Sector 33-IB-C and Sector 33-ID beamline of the Advanced Photon Source, Argonne National Laboratory, USA. The high flux from the synchrotron X-ray source delivered at this beamline allows one to detect the weak diffracted intensities arising from the lattice modulations associated with the polar vortex present in the superlattices (Fig. 1a). The double crystal monochromator, in conjunction with two mirrors, was used to deliver a highly monochromatic beam with negligible contamination from higher harmonics. Moreover, the excellent angular accuracy of the Huber 4-circle diffractometer at Sector 33-IB-C and Newport 6-circle diffractometer (20keV) at Sector 33-ID allows us to determine the orientation of our crystals very reliably, and to obtain 3D RSMs with high

accuracy. Lastly, the availability of the PILATUS 100K pixel detector is essential for the efficient acquisition of 3D RSMs.

Electron paramagnetic resonance analysis. The main EPR spectra in Fe-$PbTiO_3$ thin films and the superlattice were measured at 5 K, using a Bruker EMX plus EPR spectrometer at frequency 9.4 GHz. Some measurements were also carried out using a Varian E109 spectrometer equipped with a Model 102 microwave bridge. The spectrometer conditions used were as follows: microwave frequency, 9.23GHz, field modulation amplitude, 32G at 100kHz and microwave power, 20mW.

EPR spectra were interpreted by using spin Hamiltonian of the general form for Fe^{3+} ion ($3d^5$, S = 5/2) in the orthorhombic symmetry:

$$\mathbf{H} = \frac{1}{3} DO_2^0 + \frac{1}{180} FO_4^0 + \frac{1}{120} a\left(O_4^0 + 5O_4^4\right) + EO_2^2 + G_z H_z S_z + G_x H_x S_x + G_y H_y S_y, \quad \text{(s1)}$$

with $G_i = \beta g_i$ and the usual definitions of the O_l^m operators. Here D and F parameters correspond to axial (tetragonal) crystal fields of the second and fourth degree, respectively, with the z-axis chosen along the direction of the axial crystal field, *i.e.* along the tetragonal c-axis. E is rhombic symmetry crystal field parameter and a is the cubic crystal field splitting parameter. The zero-field splitting parameters determined for bulk crystal at low temperatures (T < 20 K) have the following values: D = 1.18 cm^{-1}, a = 0.056 cm^{-1}, and F = -0.094 cm^{-1}. [1,2] g factor is almost isotropic: g_z = 2.010 and $g_{x,y}$ = 2.009. Because the largest contribution to the energy splitting comes from the tetragonal term, $D >> G_i$, perturbation theory can be used for calculation of resonance fields for the 1/2 ↔ -1/2 central transition as only this transition is measurable in $PbTiO_3$ films. The corresponding expression for the effective g factor is the same as that obtained for the Fe^{3+} - V_O center in $SrTiO_3$[3]:

$$g_{ef} = \left(g_z^2 \cos^2\theta + 9g_\perp^2 \sin^2\theta\right)^{0.5}\left(1 - \frac{2\left(g_\perp \beta H\right)^2}{(2D_e)^2} F(\theta)\right) - \frac{36E}{D_e} Sin^2\theta \frac{g_x^2 \cos^2\delta - g_y^2 \sin^2\delta}{\left(g_z^2 \cos^2\theta + 9g_\perp^2 \sin^2\theta\right)^{0.5}}, \quad \text{(s2)}$$

$$g_\perp^2 = g_x^2 \cos^2\delta + g_y^2 \sin^2\delta,$$

where $2D_e = 2D - \frac{5}{2}a - \frac{5}{3}F,$

$$F(\theta) = \sin^2\theta\left(\frac{\left(9g_\perp^2 + 2g_z^2\right)\sin^2\theta - 2g_z^2}{\left(9g_\perp^2 - g_z^2\right)\sin^2\theta + g_z^2}\right).$$

Here θ and δ are the polar and azimuthal angles of H with respect to the main axis z of the center which coincides with the c-axis of actual domain. One can see that at the condition $D >> g\beta H, E, F, a$, resonance field of the central transition changes from $g_{eff} = g_z = 2.010$ at $H//c$ to $g_{eff} \approx 3g_\perp \approx 6$ at $H \perp c$. Because we obtained approximately the same g factors as in bulk material in $PbTiO_3$ films, one can conclude that the crystal field parameters in films do not markedly differ from those measured in bulk crystals. The expression (s2) can be thus used for analysis of the Fe^{3+} spectra in films as well. In particular, the D constant in Fe-$PbTiO_3$/$SrTiO_3$ superlattices can be estimated from measured $g_{eff} = 5.944$. It is ≈ 0.6 cm^{-1}, almost two times smaller than that in bulk crystal, indicating on smaller c/a ration in film.

Based on the relation between magnetic anisotropy energy and D term,[4] the anisotropy constant $K_{u1} = -5D$ is of -370 μeV at $T = 0$ K, where the negative value means that the tetragonal c-axis is the hard axis for Fe^{3+} spins in Fe-$PbTiO_3$/$SrTiO_3$ superlattices. In reality, this anisotropy constant will be smaller as rhombic components of crystal field were not taken into account. Thus, the spin easy axis lays in the perpendicular plane in agreement with DFT calculations. Its actual position is determined rhombic components of crystal field.

Scanning transmission electron microscopy. Determination and mapping of the polar atomic displacements ($\boldsymbol{P}_{PD}$) was performed on the atomic-scale HAADF-STEM images by

using each titanium and lead atom column offsets measured from the atom position fitting of the titanium and lead atoms. The atom positions were determined by fitting them as 2D Gaussian peaks using Matlab. The titanium displacement in each $PbTiO_3$ unit cell was calculated as a vector between each titanium and the center of mass of its four nearest lead neighbors. The displacement of the titanium in each unit cell is opposite to the polarization direction of the Fe-$PbTiO_3$. The visualization of the 2D polar displacement vectors was carried out using Matlab. Random noise in the displacement vector maps was reduced by a weighted smoothing length of 1.2 nm.

Density functional theory calculations. A polar vortex formed in 8-layers $PbTiO_3$/8-layers $SrTiO_3$ was represented in a 16x1x16 supercell, with atomic coordinates obtained from second principles calculations carried out in a previous work.[5] The magnetocrystalline anisotropy energy (MCAE) was calculated using density functional theory (DFT) for an isolated Fe^{3+}-dopant on each of the Ti-sites in the $PbTiO_3$ layers. For each Ti-site, the local environment was extracted from the 16x1x16 supercell and set up in a 3x3x3 supercell (135 atoms) with the isolated Fe^{3+}-dopant at the center and the average ion positions at the edges used to generate periodic boundary conditions. It was assumed that the Fe^{3+}-dopant would follow the Ti-ion displacement in the vortex structure, therefore the structure was frozen.

The DFT calculations were carried out using the Vienna *Ab-initio* Simulation Package (VASP)[6,7,8,9] with projector augmented wave pseudopotentials[10,11] including Pb $5d^{10}6s^26p^2$, Sr $4s^24p^65s^2$, Ti $3s^23p^63d^24s^2$, Fe $3d^64s^2$ and O $2s^22p^4$ electrons as valence. The PBEsol functional was used with a plane wave cut-off energy of 750 eV and a 2x2x2 Gamma-centered *k*-point grid, which converged the total energy to 1 meV per formula unit. In each 3x3x3 supercell one Ti out of 27 was replaced with an Fe ion, and one electron was added to correctly compensate

the Fe^{3+} charge state ($Fe_{Ti}^{'}$). The Fe-Fe distance of ~ 11.6Å ensured that the dopant ions were sufficiently isolated from each other. An effective Hubbard term $U_{eff} = U - J = 4$ eV was added to the Fe *d*-orbitals within the Dudarev approach.[12] We have previously noted that the exchange-correction (*J*) parameter does not affect the spin easy direction in this material.[13] The magnetocrystalline anisotropy was calculated by including spin-orbit coupling self-consistently and varying the spin quantization axes over 26 directions. The MCAE surface was fitted to the energy for each of the 26 directions and the spin easy axis was taken as the principal axis with the largest MCAE.

REFERENCES

[1] Sandhya, S et al, Atomic scale crystal field mapping of polar vortices in oxide superlattices, *Nat. Comms.* **12**, 1-7 (2021)

[2] Warren, W. L., Dimos, D., Pike, G. E., Vanheusden, K. & Ramesh, R. Alignment of defect dipoles in polycrystalline ferroelectrics. *Applied Physics Letters* **67**, 1689-1691, (1995).

[3] von Waldkirch, T., Müller, K. A. & Berlinger, W. Analysis of the Fe^{3+}-V_O Center in the Tetragonal Phase of $SrTiO_3$. *Physical Review B* **5**, 4324-4334, (1972).

[4] Fuchikami, N. Magnetic Anisotropy of Magnetoplumbite $BaFe_{12}O_{19}$. *Journal of the Physical Society of Japan* **20**, 760-769, (1965).

[5] Aguado-Puente, P., & Junquera, J. (2012). Structural and energetic properties of domains in PbTiO 3/SrTiO 3 superlattices from first principles. Physical review B, 85(18), 184105.

[6] Kresse, G. & Hafner, J. *Ab initio* molecular dynamics for liquid metals. *Physical Review B* **47**, 558-561, (1993).

[7] Kresse, G. & Hafner, J. *Ab initio* molecular-dynamics simulation of the liquid-metal--amorphous-semiconductor transition in germanium. *Physical Review B* **49**, 14251-14269, (1994).

[8] Kresse, G. & Furthmüller, J. Efficient iterative schemes for *ab initio* total-energy calculations using a plane-wave basis set. *Physical Review B* **54**, 11169-11186, (1996).

[9] Kresse, G. & Furthmüller, J. Efficiency of *ab-initio* total energy calculations for metals and

semiconductors using a plane-wave basis set. *Computational Materials Science* **6**, 15-50, (1996).

[10] Blöchl, P. E. Projector augmented-wave method. Physical Review B **50**, 17953-17979, (1994).

[11] Kresse, G. & Joubert, D. From ultrasoft pseudopotentials to the projector augmented-wave method. Physical Review B **59**, 1758-1775, (1999).

[12] Dudarev, S. L., Botton, G. A., Savrasov, S. Y., Humphreys, C. J. & Sutton, A. P. Electron-energy-loss spectra and the structural stability of nickel oxide: An LSDA+U study. *Physical Review B* **57**, 1505-1509, (1998).

[13] J. Liu, V. V. Laguta, K. Inzani, W. Huang, S. Das, R. Chatterjee, E. Sheridan, S. M. Griffin, A. Ardavan, and R. Ramesh, *Science Advances* **7**, eabf8103 (2021).

Supplementary Figures

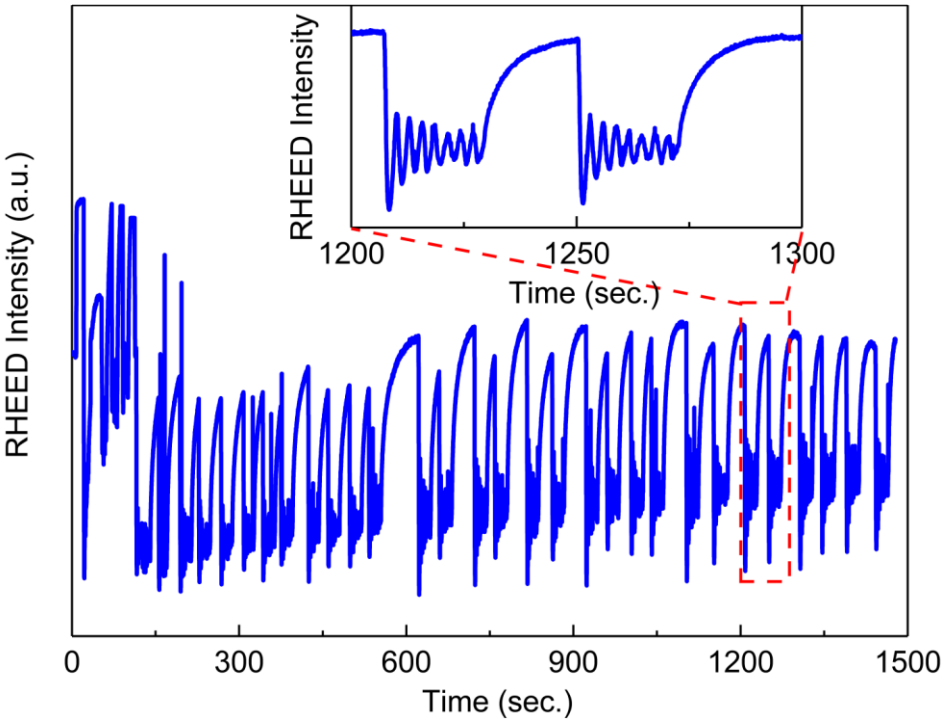

S1| RHEED-controlled growth of Fe-$PbTiO_3$ single layer. RHEED oscillations present throughout the growth of the 100-nm-thick Fe-$PbTiO_3$. The insert shows the zoom out of 2 sets of 8 unit cell oscillations.

To check if the $PbTiO_3$ lattice is flexible (or compliant) with respect to ionic shifts along a direction perpendicular to the *c*-axis, we performed measurements on a single crystal under application of electric field at different directions (Supplementary Figure 2). The upper spectrum is the initial spectrum measured at magnetic field direction $\theta=25^0$ before application of electric field at [010] direction. The strong line originates from domains oriented along [001] direction. When the electric field is applied at [010] direction, domains start to align along the *E*-field, which is reflected in disappearance of the line at *H*=2150 G and appearance of the line at 1225 G. However, the strength of the electric field is not sufficient enough to achieve complete switching of polarization and there are still crystal regions with *c*-axis oriented along the initial [001] direction. The spectral line from these regions is shifted to higher fields with respect to the initial resonance field H_r=2150 G and this shift increases with an increase of the *E*-field. If the *E*-field is changed to the opposite direction, i.e. along the [0-10] axis, this line shifts to lower magnetic fields. It also splits into two components indicating that domains with polarization in the [001] direction become inequivalent due to strains induced by 180^0 repolarization of the crystal. The observed shift of resonance lines is surely related to deviation of the Fe^{3+} magnetic axis from the [001] crystal axis induced by electric field as the shift is proportional to dH/dθ. Also, this shift of spectral line in electric field is not related to the piezo effect because the 1/2 ↔ -1/2 central transition is insensitive to small lattice deformations. The deviation angle $\Delta\theta$ in electric field can be roughly estimated from the following simple relation $\Delta H_r = \frac{dH_r}{d\theta}\Delta\theta$, where ΔH_r is the shift of resonance field in electric field. This gives $\Delta\theta$=3.2^0. Thus, our data confirm the principal possibility of local polarization rotation in $PbTiO_3$ even by small electric fields. Because internal electric fields (depolarization fields) in Fe-

$PbTiO_3/SrTiO_3$ superlattices must be much larger than 30 kV/cm, much larger rotations of polarization are expected.

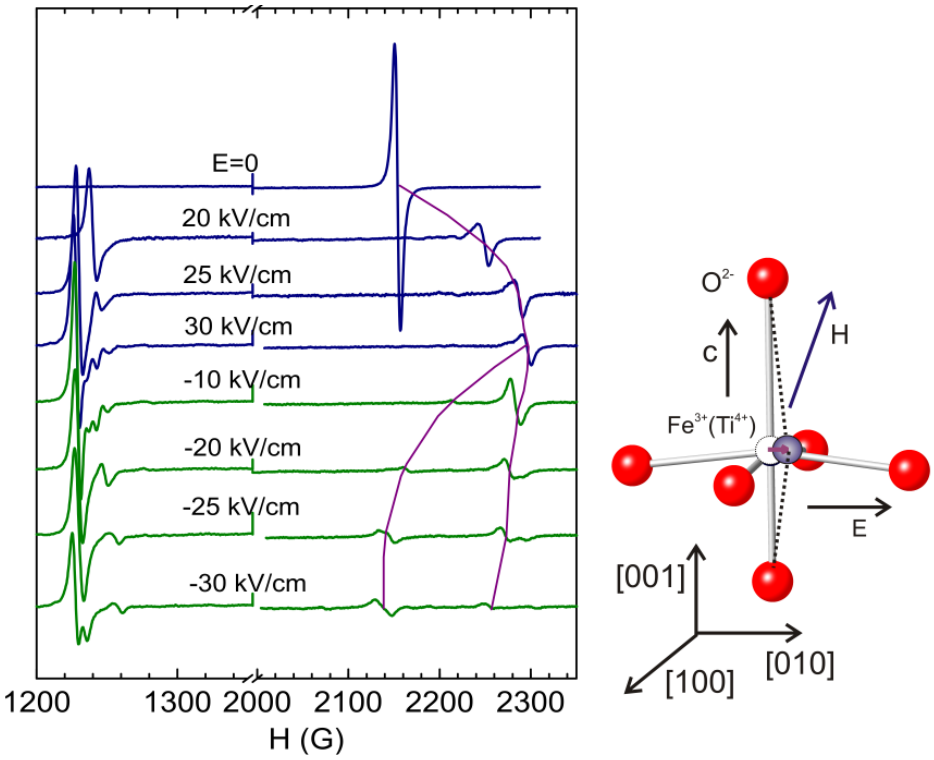

S2| Dependence of Fe^{3+} EPR spectrum in $PbTiO_3$ crystal under application of electric field at direction perpendicularly to *c*-axis. The spectra were measured at at the magnetic field direction $\theta = \angle(\mathbf{c},\mathbf{H})=25^0$. The insert shows simplified local ionic reconstraction of oxygen octahedron.